J. Appl. Comput. Mech., 3(4) (2017) 283-292
DOI: 10.22055/JACM.2017.21992.1122

ISSN: 2383-4536
jacm.scu.ac.ir

Shahid Chamran University of Ahvaz

Journal of Applied and Computational Mechanics

Research Article

Finite Element Analysis for CFST Columns under Blast Loading

Peyman Beiranvand[1], Fereydoon Omidinasab[1], Marziye sadate Moayeri[2], Shahpoor Mehdipour[3], Mohammad Zarei[4]

[1] Department of Civil Engineering, Lorestan University, Khorram abad, Iran
[2] Lecturer, Civil engineering faculty, Borujerd Branch, Islamic Azad University, Iran
[3] Department of Civil Engineering, Arak Brunch, Islamic Azad University, Iran
[4] PhD Candidate, Department of Civil engineering, Imam Khomeini international university, Qazvin, Iran

Received October 12 2016; Revised April 14 2017; Accepted for publication June 20 2017.
Corresponding author: Peyman Beiranvand, Peyman51471366@gmail.com

Abstract. The columns of frame structures are the key load-bearing components and the exterior columns are susceptible to attack in terrorist blasts. When subjected to blast loads, the columns would suffer a loss of bearing capacity to a certain extent due to the damage imparted which may lead to their collapse and even cause the progressive collapse of the whole structure . The concrete-filled steel columns have been extensively used in the world due to the existence of all suitable characteristics of concrete and steel, more ductility, increasing concrete confinement using the steel wall, the large energy-absorption capacity and the appropriate fire behavior. In the present study, the concrete-filled steel square columns have been simulated under the influence of the blast load using the ABAQUS software. These responses have been compared for scaled distances based on the distance to the source and the weight of the explosive material. As a result, it can be seen that although concrete deformation has been restricted using the steel tube, the inner layer of concrete has been seriously damaged and the column displacement has been decreased by increasing the scaled distance. We also concluded that the concrete-filled steel columns have the high ductility and the blast resistance.

Keywords: Blast load; Concrete-filled steel columns; Finite element analysis.

1. Introduction

The concrete-filled steel tube (CFST) columns have been widely used in engineering structures such as high-rise buildings, arch bridges, and factories since they enjoy advantages of the high strength and the excellent ductility due to a confinement effect and a changed buckling mode [1,2]. As a result of increasing terrorist bombings in recent years, the blast resistance of the structures has become a consideration in the design process [3]. When subjected to blast loads, the columns may suffer a loss of bearing capacity to a certain extent due to the damage imparted which may induce the collapse of the columns and even cause the progressive collapse of the whole structure. In addition, both concrete and steel, of which the CFST columns are composed, may respond to the blast loads at very high strain rates in the order of 1–100 s−1 or even higher, and thus, make the dynamic analysis of the CFST columns different from that under the static loads and the earthquake actions. Therefore, it is of a realistic significance to study the dynamic behavior and damage characteristics of the CFST columns under the blast loading.

Nowadays, the concrete-filled steel structures have been extensively used all around the world due to their more economic characteristics, less deformation in the lateral loading, reduction in the dimensions of the section with the same load capacity and the less weight; in other words, they possess all suitable characteristics of concrete and steel. These types of sections also

Published Online: June 20 2017

include the ductility, the larger energy absorption capacity and the power and ultimately the fire resistance. Explosion is the result of the sudden release of energy in the form of combusting gases and the nuclear explosion or as the result of different types of bombs. TNT is usually used as a reference for determining the explosion power. Among the main characteristics of explosion that leads to pushing force on the structure, we might refer to the randomness of the explosive situation, the forces' dynamicity and the transience of forces and the low impact (ranging from a few milliseconds to several seconds). When an explosion happens, the energy is suddenly released. The effect of releasing this energy can be divided into two types of the thermal radiations and the wave propagation in the land and the air, however, the present study investigates only the first type. The steel is a material with a high thermal lead, however, when it is affected by the fire, its resistance is rapidly decreased. The blast responses are usually more noticeable for vital structures and protection ones. By loading the concrete-filled steel columns, the restricted concrete prevents the local buckling to penetrate the steel wall because there will be the restriction mood in the concrete, and therefore, it will be pressured triaxially and the member's rapture will be deformed from the brittle state to plastics as compared to the concrete columns.

Fujikura et al. experimentally investigated the dynamic responses of the CFST bridge pier column specimens under the blast loading. According to the magnitude of the support rotation, the damage states of the column specimens were categorized into three types including the plastic deformation, onset of the fracture, and the post fracture. The authors also compared the maximum response of the specimens obtained from the simplified method based on the equivalent single-degree-of freedom (SDOF) theory with the test data as mentioned in [4, 5]. Li et al. studied the dynamic behavior of the CFST columns through a series of the field blast experiments. They analyzed the effects of the explosive mass, the standoff distance, the axial load ratio, the concrete strength grade, and the steel ratio on the displacement and strain responses of the CFST columns which showed global-mode controlled responses in the tests [6]. Remennikov and Uy carried out field tests on the CFST specimens and demonstrated the effects of the scaled standoff distance on the mode of response and failure of the specimens under the near-field blast loading. It was found that the CFST members may suffer a severe localized damage due to the highly localized blast impulse when the explosive was located quite close to the test members. The authors also developed a simplified engineering-level model for the prediction of the mid-span deflection history of the CFST member [7]. Ngo et al. utilized the coupled Arbitrary Lagrange Euler (ALE) blast wave-structure interaction algorithms and numerically investigated the failure patterns, deformation histories, and energy absorption characteristics of the CFST members subjected to the near-field blast loading. Two distinct phases of the deformation process were identified in the study of which the local deformation that initially occurred rather than the followed flexural global deformation dominates the energy absorption history of the column specimen [8]. Zhang et al. carried out blast tests and finite element simulations on the axially compressed CFST column members. Results indicated that the CFST columns showed a good resistance against flexural loads under the blast loading. The energies absorbed by the local and flexural deformations of the column during the blast loading were also investigated, and it was found that the majority of the energies were absorbed by the global deformation when the mode of response was mainly flexural [9]. The authors also investigated the dynamic responses and damage characteristics of the concrete-filled columns with double-skin tubes to blast loads, and the critical parameters that affect the displacement time histories of the columns were analyzed [10]. The review of literature indicates that the mode of the response and damage criterion are key issues in understanding the dynamic behavior and damage characteristics of CFST columns subjected to blast loads while some damage criterions are only applicable to certain damage modes of the columns and different conclusions may be drawn under varied damage modes as stated previously. The aim of this study is to examine the damage modes and damage assessment of the CFST columns under the blast loading. The numerical model is established by using the finite element program LS-DYNA and calibrated with correlated experimental studies by other researchers. Moreover, the possible damage modes of the columns subjected to the blast loads are analyzed and the suitable criterion for assessing the degree of the columns damage is adopted accordingly. The parameters that may affect the damage degree of the columns are analyzed in this study including the blast condition, the column dimension, the steel ratio, and the axial load ratio which are then incorporated into a proposed equation that is capable of estimating the damage degree of the CFST columns based on the numerical results.

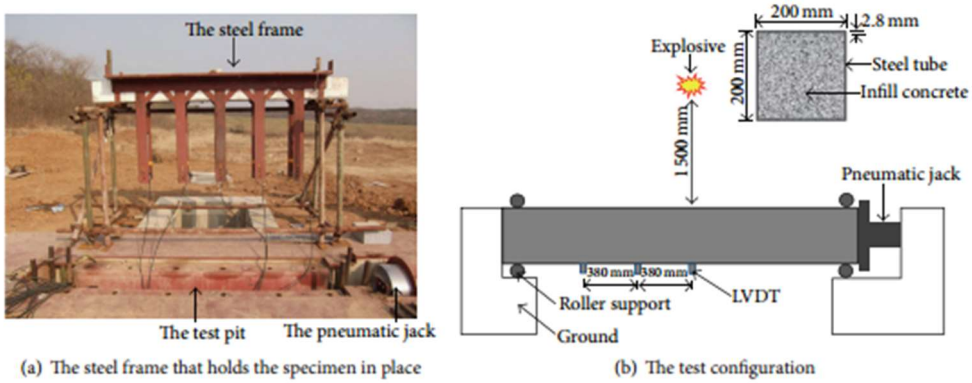

Fig. 1. Test setup (Zhang et al. [9])

2. Characteristics of the concrete and steel features

The thermal and mechanical characteristics of the steel and the concrete are completely different from each other; however, by increasing the temperature, the resistance and stiffness of both will be decreased. The stress-strain curves of the steel and the concrete for normal temperature (20 degrees Celsius) are shown in Figures 2 and 3 as T20. For all sections of this study, the obtained stress (f_y) equals to 350 newton per square millimeter, the modulus of elasticity (E_s) equals to 21 × 104 newton per square millimeter, the compressive resistance (f_c) equals to 30 newton per square millimeter and the strain (ε_c) equals to 0.0025. The stress-strain curve of the steel is affected by increasing the temperature based on regulation of BS EN 1993-1-2 [11] and for the concrete is based on -BS EN 1994-1-2 [12].

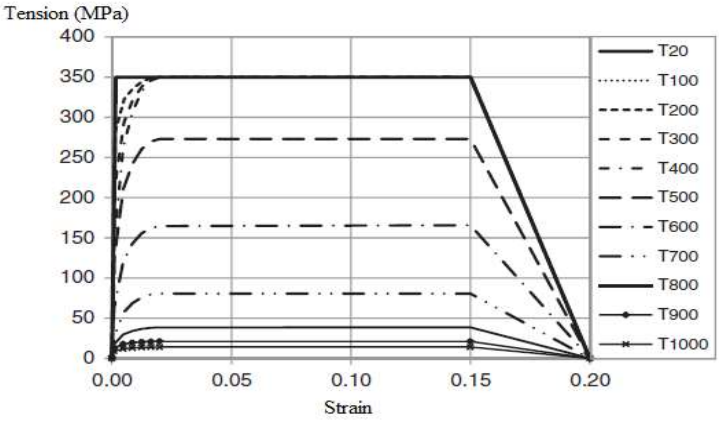

Fig. 2. Stress-strain curve of the steel affected by increasing the temperature [11]

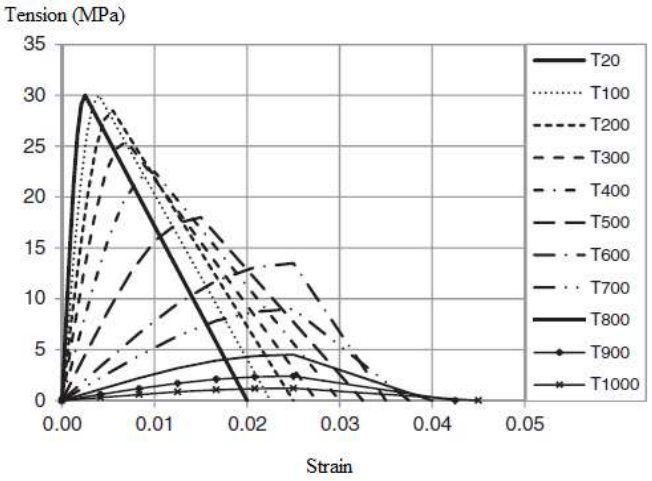

Fig. 3. Stress-strain curve of the concrete affected by increasing the temperature [12]

For simulation by using ABAQUS [13], the steel is modeled based on the real stress-strain relationship that is obtained from equations 1 and 2.

$$\sigma_{true} = \sigma_{nom}(1+\varepsilon_{nom}) \tag{1}$$

$$\varepsilon_{true} = \ln(1+\varepsilon_{nom}) \tag{2}$$

In which, σ_{nom} and ε_{nom} are the nominal strain and stress of the section, respectively. The real values of stress and strain of the steel are shown in Table 1.

Table 1. Real values of steel strain-stress

Plastic strain	Real stress (MPa)
0.000	300
0.025	350
0.100	375
0.200	394
0.350	400

For modeling the concrete in the plastic area and investigating its destruction, the concrete plastic damage model is used. The values of stress, strain and destructing concrete plastic in tension and compression are presented in Tables 2 and 3.

Table 2. Values of stress, strain and destruction of the concrete plastic in tension

Destruction in stretch parameter	Cracking strain	Tensile strength (MPa)
0.00	0.000000	5.3
0.25	0.000176	5.31
0.99	0.001539	0.58

Table 3. Values of stress, strain and destruction of the concrete plastic in compression

Destruction in stretch parameter	Cracking strain	Tensile strength (MPa)
0.000	0.000000	17.5
0.112	0.00038	25.7
0.429	0.00189	34.9
0.466	0.00218	35
0.701	0.00456	38

3. Finite element materials models

3.1 Blast load modeling

As it can be seen in Figure 4, the blast loading happens in a determined distance from the structure (R). The structure's height is 3 meters and the dimensions of the column is 500×500 and the thickness is 10 millimeter.

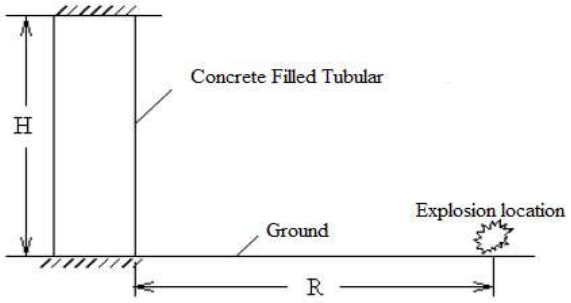

Fig. 4. Concrete-filled steel column under the blast load

3.2 Numerical simulation by ABAQUS software

The concrete-filled steel structures are first modeled in the ABAQUS software the same as Figures 5 and 6.

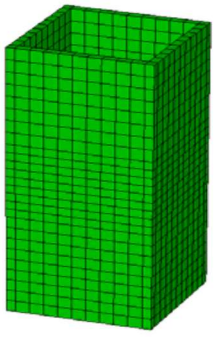

Fig. 5. Finite element model of the steel wall in concrete-filled steel columns

The plastic analysis includes three main components of the strain-stress curve which yields the criterion and the hardening law. The strain-stress curve for structural components is mentioned in the second section. For modeling materials' behavior, the Von Mises which yields the criterion and the isotropic hardening law are used. The problems related to the geometric non-linear analysis are also considered in this model and the large deformations method is used. The analysis method is the Newton-Raphson software. The reason for the selection of this method is the contacting elements between the concrete and the steel and the consideration of contact surfaces friction. Therefore, the non-symmetric Newton-Raphson method is used. The concrete core is defined by a three-dimensional element of eight nodes and with three degrees of freedom at each node using the C3D8R model. The materials are concrete-type with the capability of the cracking in three orthogonal lengths under the tensile and fracture, pressure strains as well as plastic deformations.

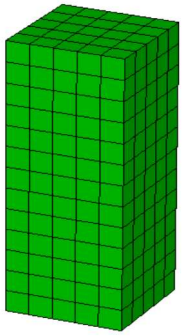

Fig. 6. Finite element model of the concrete core in concrete-filled steel columns

The steel wall is defined by the C3D8I element that is defined the same as the C3D8R element with eight nods and three degrees of freedom at each nod and a good agreement with other utilized elements in the model. The friction and the slip between the steel and the concrete core are also modeled by a surface to surface contacting element. This element is able to transfer the pressure toward the normal length and shear as well as desired surfaces tangent. To investigate the behavior after the column buckling and the passing critical point and to show the decrease in the loading capacity without divergence in problem-solving, the arc length method is used for solving non-linear equations.

For modeling the blast load, existing equations in the TM5-1300 regulation [14] are used. This regulation is extensively used for primary designing of the structures under the blast loading. The scaled distance is calculated from the third root of different distances to the blast load weight that is shown in Equation 3.

$$z = \sqrt[3]{\frac{R}{W}} \tag{3}$$

where R is the distance from the blast source and W is the weight of the blast load. As it can be seen in Figure 7, the time-pressure diagram is shown in which the point of $0.1 < P_{s0} < 10$ represents the time of the reaching blast wave to the structure. Consequently, the pressure reaches to its most value that is P_{s0}, then the amount of the applied pressure is reduced and reaches the amount of the environmental pressure P_0; till this moment, the pressure is in a positive phase. The corresponding time to a pressure negative phase with t_0^- and the maximum amount of the negative pressure is shown with P_{s0}^- [15].

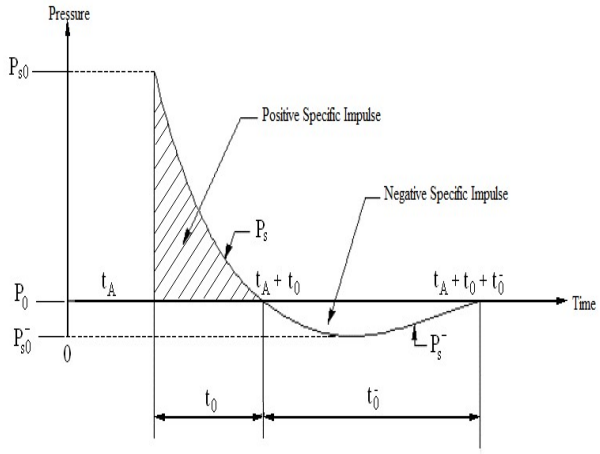

Fig. 7. Variation of the overpressure with the distance at a given time from the center of explosion

The pressure negative phase, as compared to the positive one, is usually less important for designing. In other words, only the pressure positive phase is considered for the numerical simulation of the blast load. The empirical formula of the time-pressure is shown in Equation 4.

$$P(t) = P_{s0}\left(1 - \frac{t}{t_0}\right)\exp\left(\frac{-bt}{t_0}\right) \tag{4}$$

where b is a parameter of the blast wave. The equation of the maximum amount of the blast load P_{s0} is calculated based on the scaled distance z by Brode [16] in 1955. This value is shown in Eqs. (5-a) and (5-b).

$$P_{s0} = \frac{0.975}{z} + \frac{1.455}{z^2} + \frac{5.85}{z^3} - 0.019 \quad bar \qquad 0.1 < P_{s0} < 10 \tag{5a}$$

$$P_{s0} = \frac{6.7}{z^3} + 1 \quad bar \qquad P_{s0} > 10 \tag{5b}$$

On the other hand, Newmark [17] in 1961 proposed another Equation for the maximum blast load that is shown in Equation 6.

$$P_{s0} = 6784\frac{W}{R^3} + 93\left(\frac{W}{R^3}\right)^3 \tag{6}$$

The blast waves are propagated at the supersonic speed and ultimately they are collided with the structure. After colliding with structure, these waves are intensified with an extra pressure. This subject, which is considered in the TM5-1300 regulation, is shown in Equations 7 to 11. Due to the very short time of loading, the load derived from explosion has an impact nature; therefore, the time-based pressure changes are considered as linear in many cases.

$$q_0 = \frac{2.5P_{s0}^2}{7P_{s0} + P_0} \tag{7}$$

$$P_R = P_{s0}\left[2 + \frac{6P_{s0}}{7P_0 + P_{s0}}\right] \tag{8}$$

$$t_d = 20.77\left[\frac{W}{P_{s0}}\right]^{1/3} \qquad P_{s0} < 2 kg/cm^2 \tag{9a}$$

$$t_b = 14.35\left[\frac{W}{P_{s0}}\right]^{1/3} \qquad P_{s0} \geq 2\ kg/cm^2 \tag{9b}$$

$$t_b = 10.23\left[\frac{W}{P_{s0}}\right]^{1/3} \qquad P_{s0} < 70\ kg/cm^2 \tag{10a}$$

$$t_b = 20.77\left[\frac{W}{P_{s0}}\right]^{1/3} \qquad P_{s0} \geq 70\ kg/cm^2 \tag{10b}$$

$$t_c = \frac{3s}{v} < t_d, \quad v = \left[1 + \frac{6P_{s0}}{7P_0}\right] \tag{11}$$

The diagram of the time-based pressure changes which are caused by the explosion on different dimensions of structure is presented in Figures 8, 9 and 10. The pressure changes are provided for the front face (toward explosion) of the structure, the side face, the roof and for the behind explosion.

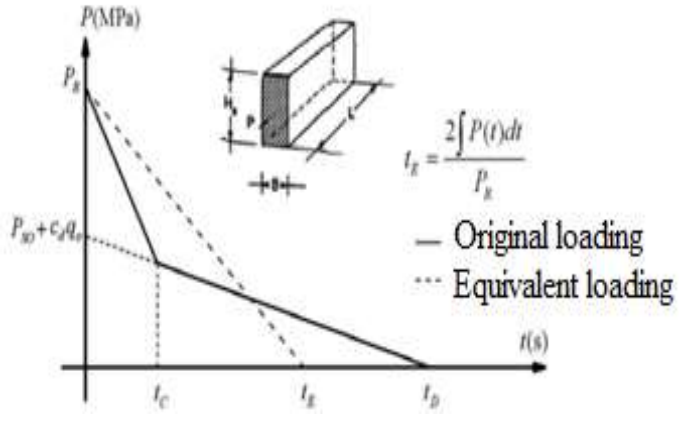

Fig. 8. Pressure changes on the front face (toward structure) of the structure

The distance from the source of explosion (R) is 5 meters and the scaled distance (Z) is considered as 0.7, 1 and 1.3. The blast pressure is considered as the uniform load over the surface of the column. This numerical simulation is implemented in order to evaluate the blast responses and the damages of the concrete-filled steel columns under blast loads.

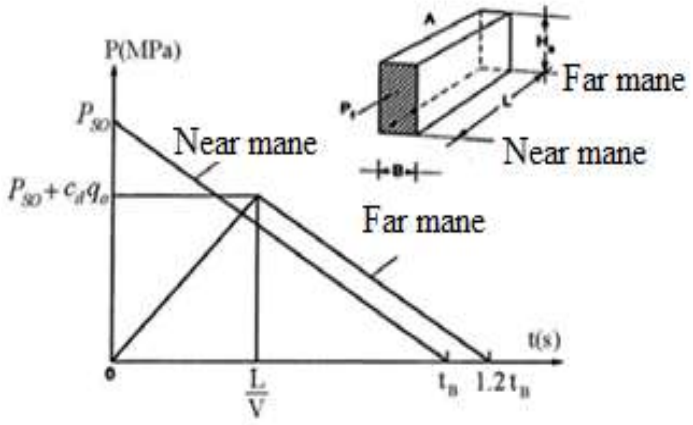

Fig. 9. Pressure changes on the side faces and the roof of the structure

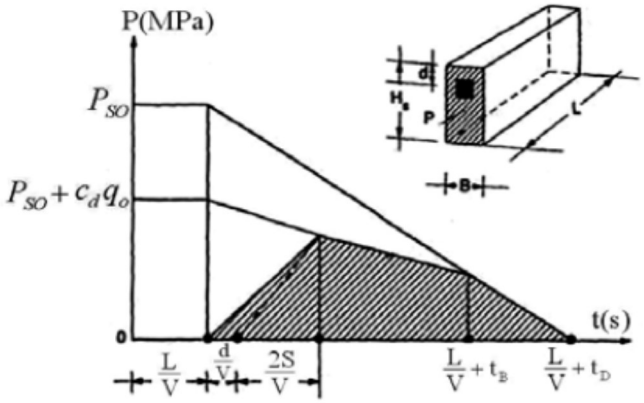

Fig. 10. Pressure changes on the behind face of the structure

4. Results

4.1 Investigating numerical results for z=1

Displacement values in direction x and the maximum main stress in times 2, 5 and 9 millisecond are presented in Figures 11 to 13. As it can be seen, the maximum displacement happens in the middle of the column. This subject is expected because the column has symmetric reliance and is under the uniform loading and the maximum displacement should naturally happen in the middle of the span. The displacement is increased to 117 millimeters by increasing the time to 9 milliseconds. In terms of the stress, it can also be seen that the first tensile damage is happened upside and downside of the concrete and the main maximum stress becomes equal to the concrete tensile resistance. When the time increases to 9 milliseconds in the middle column concrete, the damage and the erosion happen simultaneously. However the ratio of the displacement to the height of the column equals to 3.9 percent, it can be concluded that the steel section effectively causes restricting lateral displacement of the column and increases the column resistance against the explosion.

4.2 Comparing numerical results for z=0.7 and z=1.3

The diagram of displacement in the direction x column is presented in Figure 14 for scaled distances of 0.7 and 1.3. As it can be seen, the maximum displacement of the column decreases by increasing scaled distances.

It can also be observed that contrary to ordinary columns where after reaching the maximum load, the loading capacity severely decreases and there is no tolerance for the large displacement in levels close to the maximum load, after reaching the maximum load, the concrete-filled steel columns experience a very low decrease in the loading capacity and tolerate the large displacement well in levels close to the maximum load.

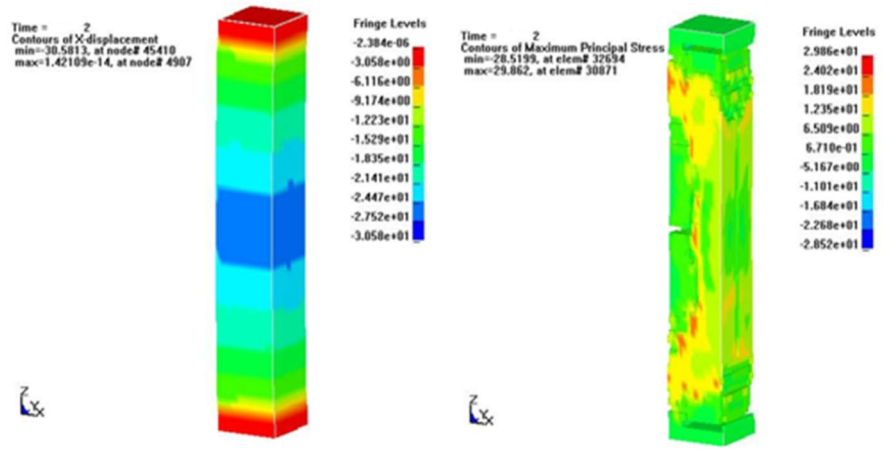

Fig. 11. Displacement and stress in 2 milliseconds

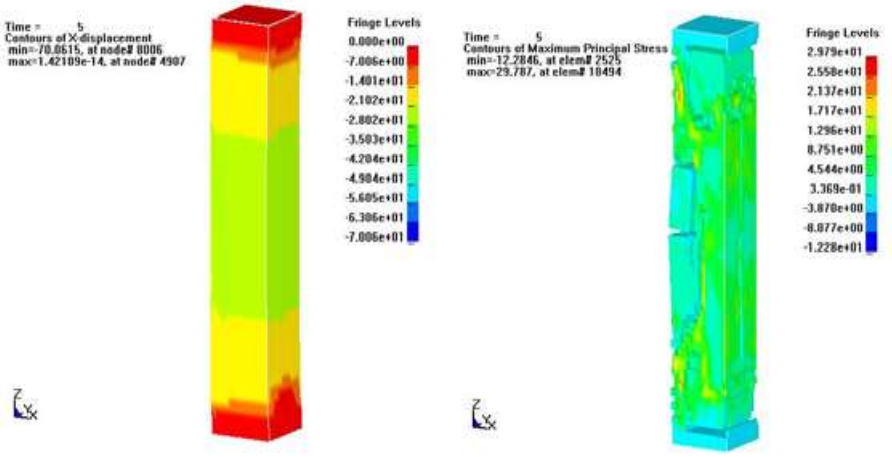

Fig. 12. Displacement and stress in 5 milliseconds

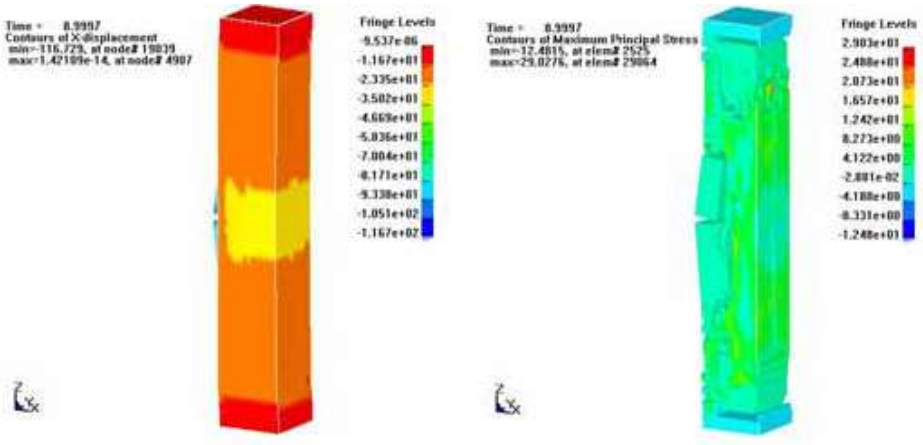

Fig. 13. Displacement and stress in 9 milliseconds

As a result, it can be stated that for modeling the loads caused by explosion, concentrated loads in levels of floors with linear distribution toward time can be used since they have adequate accuracy and their error level, compared to the extensive load with the nonlinear distribution of time in low rise buildings, is less than 10 percent and in tall buildings is about 10 percent. The blast effect on structural components that are closer to the explosion location is absolutely more severe. This means that the most important vulnerable points against blast loads are external structure components and these components are more exposed to damage than other ones. The loads caused by explosion create relatively high shearing power in columns close to the blast; this force is decreased in the columns of next rows.

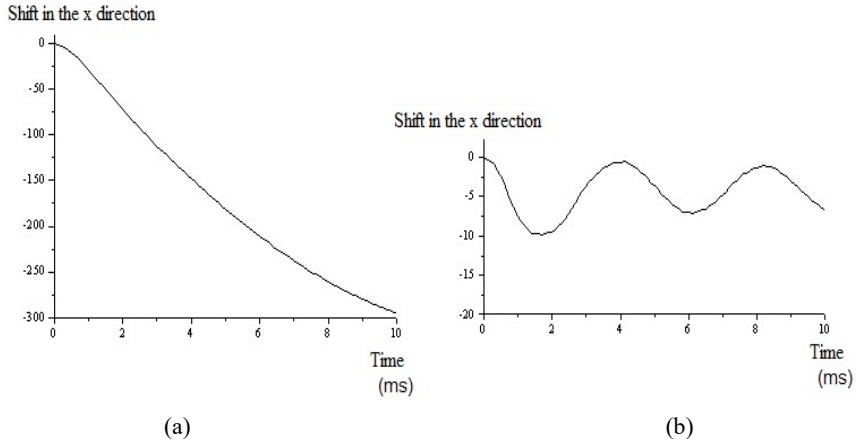

Fig. 14. Comparing the displacement diagram for (a) z=0.7 and (b) z=1.3

Increasing the number of frame openings doesn't significantly affect created force in the column in first row but it causes reducing the general lateral displacement of the frame. On the other hand, by increasing the floors, the created force in columns of low floors of building is not increased to a great extent; therefore, short buildings are vulnerable toward blast loads out of the structure due to high forces caused by the blast in them, compared to normal designing forces of high buildings. Therefore, in order to have an appropriate design against explosive loads, external structural components should be carefully considered. The columns and structural components in the first floor are also double important and as a recommendation, we can say that designing the structure is better to be controlled through eliminating one of external columns in the first floor.

5. Conclusions

This study presents a 3D numerical model to the finite element analysis for CFST columns under the blast loading. The flexural and shear damages of the column are mainly attributed to the deformation and the internal force of the whole member, whilst the localized damage is dominated by the failure of the infill concrete and the steel tube in the vicinity of the explosion.

Based on the numerical analysis results, the following conclusions can be drawn. The maximum displacement in the column will decrease by increasing scaled distances. The columns are the most important factors in determining the lateral behavior of moment frames under external blast loads. The steel section will effectively lead to the restricting column lateral displacement and increasing the column resistance against the explosion. By increasing the dimensions of columns, the relative displacement of floors will change less but they will not be decreased necessarily. Increasing the aspects of around columns affects the lateral displacement by reducing rather than increasing the dimensions of inner columns. When the time increases up to 9 milliseconds, in the middle concrete of the column, the damage and the erosion will occur simultaneously.

References

[1] Choi, Y.-H., Foutch, D.A., LaFave, J.M. New approach to AISC P-M interaction curve for square concrete filled tube (CFT) beam–columns,Engineering Structures, 28(11), 2006, pp. 1586–1598.

[2] Choi, Y.-H., Kim, K.S., Choi, S.-M. Simplified P-M interaction curve for square steel tube filled with high-strength concrete, Thin-Walled Structures, 465, 2008, pp. 506–515.

[3] Krauthammer, T. Modern Protective Structures, Taylor & Francis Group, New York, NY, USA, 2008.

[4] Fujikura, S.C., Bruneau, M., Lopez-Garcia, D. Experimental investigation of blast performance of seismically resistant concrete-filled steel tube bridge piers, Tech. Rep. MCEER-07- 0005, University at Buffalo, Buffalo, NY, USA, 2007.

[5] Fujikura, S., Bruneau, M., Lopez-Garcia, D. Experimental investigation of multihazard resistant bridge piers having concrete-filled steel tube under blast loading, Journal of Bridge Engineering, 13(6), 2008, pp. 586–594.

[6] Li, G., Qu, H., Yang, T., Lu, Y., Chen, S. Experimental study of concrete-filled steel tubular columns under blast loading, Journal of Building Structures, 34(12), 2013, pp. 69–76.

[7] Remennikov, A.M., Uy, B. Explosive testing and modelling of square tubular steel columns for near-field detonations, Journal of Constructional Steel Research, 101, 2014, pp. 290–303.

[8] Ngo, T., Mohotti, D., Remennikov, A., Uy, B. Numerical simulations of response of tubular steel beams to close-range explosions, Journal of Constructional Steel Research, 105, 2015, pp. 151–163.

[9] Zhang, F.R., Wu, C.Q., Wang, H.W., Zhou, Y. Numerical simulation of concrete filled steel tube columns against BLAST loads, Thin-Walled Structures, 92, 2015, pp. 82–92.

[10] Zhang, F., Wu, C., Zhao, X., Li, Z., Heidarpour, A., Wang, H. Numerical modeling of concrete-filled double-skin steel square tubular columns under blast loading, Journal of Performance of Constructed Facilities, 29(5), 2015, B4015002.

[11] BS EN 1993-1-2, "Euro code 3: design of steel structures, Part 1.2: General rules structural fire design", London, British Standards Institution, 2005.

[12] BS EN 1994–1–2, "Euro code 4: design of composite steel and concrete structures. Part 1.2: general rules–structural fire

design", London, British Standards Institution, 2005.
[13] ABAQUS standard user's manual, 1–3. USA: Hibbitt, Karlsson and Sorensen, Inc; 2008. version 6.8-1.
[14] TM5-1300, Structures to resist the effects of accidental explosions, US Army, USA, 1990.
[15] Bing, L., Tso-Chien, P., Anand, N. A case study of the effect of cladding panels on the response of reinforced concrete frames subjected to distant blast loadings, Nuclear Engineering and Design, 239(3), 2009, pp. 455-469.
[16] Brode, H.L. Numerical solutions of spherical blast waves, Journal of Applied Physics, 26, 1955, pp.766-766.
[17] Newmark, N.M. Protective Construction Review Guide-hardening, Defense Technical Information Center, 1961, pp. 324.